

## Auxiliary material: Text S1

### Testing morphodynamic controls on location and frequency of river avulsions on fans and deltas: Huanghe (Yellow River), China

Vamsi Ganti<sup>1</sup>, Zhongxin Chu<sup>1,2</sup>, Michael P. Lamb<sup>1</sup>, Jeffrey A. Nittrouer<sup>3</sup>, and Gary Parker<sup>4</sup>

<sup>1</sup>*Division of Geological and Planetary Sciences, California Institute of Technology, 1200 E. California Blvd., MC 170-25, Pasadena, CA 91125, USA.*

<sup>2</sup>*College of Marine Geosciences, Ocean University of China, Qingdao, 266100, China.*

<sup>3</sup>*Department of Earth Science, Rice University, 6100 Main Street, Houston, TX 77005, USA.*

<sup>4</sup>*Department of Civil and Environmental Engineering and Department of Geology, Hydrosystems Laboratory, University of Illinois, 301 N. Mathews Ave., Urbana, IL 61801, USA.*

#### 1. Sediment-transport capacity calculations

We computed the ratio of the total sediment transport capacity ( $Q_{sc}$ ) between the locations upstream and downstream of the topographic slope-break near the Huayuankou site by assuming the Engelund-Hansen relationship for total sediment load [Engelund and Hansen, 1967]:

$$Q_{sc} = w \left[ \frac{0.05}{C_f} \sqrt{RgD^3} \right] \left( \frac{\tau_b}{RgD\rho} \right)^{5/2} \quad (1)$$

where  $w$  is the active channel width,  $g$  is the gravitational acceleration,  $D$  is the grain-size,  $\rho$  is the density of water,  $\tau_b$  is the bed shear stress,  $R$  is the submerged specific density of sediment, and  $C_f$  is the dimensionless bed resistance coefficient given by

$$C_f = \frac{1}{8.1^2} \left[ \frac{H}{k_c} \right]^{-1/3} \quad (2)$$

where  $H$  is the flow-depth and  $k_c$  is a composite bed roughness coefficient. We acknowledge that equation (1) may have limited applicability to a river with a bed grain size that is close the sand-silt transition, and which is also subject to hyperconcentrated flow. With this in mind, we use it only for the purposes of a scale estimate.

Further, we computed the bed shear stress as  $\tau_b = \rho g H S$ , where  $S$  is the topographic slope. Thus, the ratio of the sediment transport capacity upstream of the slope-break to downstream of the slope-break, assuming constant grain-size and roughness coefficient, is:

$$\frac{Q_{sc1}}{Q_{sc2}} = \frac{w_1}{w_2} \left( \frac{H_1}{H_2} \right)^{17/6} \left( \frac{S_1}{S_2} \right)^{5/2} \quad (3)$$

where subscripts 1 and 2 correspond to upstream and downstream of the slope-break, respectively. In the above relation, we know the ratio of the slopes (Fig. 2 in main text), but we need to compute the ratio of widths and the flow depths upstream and downstream of the topographic slope-break.

We computed the widths of the active channel upstream and downstream of the topographic slope-break using the measure tool in Google Earth. We averaged the width of the active channel at three cross-sections each, within a 10-km window at the following locations:  $34^\circ 55' \text{ N } 111^\circ \text{ E}$  and  $34^\circ 50' \text{ N } 113^\circ \text{ E}$ . This exercise yielded average channel widths of 239 m and 713 m upstream and downstream of the topographic slope-break, respectively. We computed the ratio of the flow depths, assuming normal flow and the Manning-Strickler resistance relationship, which results in the following relation:

$$\frac{H_1}{H_2} = \left[ \frac{q_{w1}^2 S_2}{q_{w2}^2 S_1} \right]^{3/10} \quad (4)$$

where  $q_w$  is the unit water discharge. The unit water discharge upstream of the slope-break is  $\sim 3$  times that of the downstream location (because of the width variation) and combining the ratio of the slopes yields a ratio of the flow depths to be 1.1. Substituting this ratio into equation (3) yields the ratio of total sediment transport capacity at the upstream location to the downstream location to be a value of approximately 50. This value is not likely to be precisely accurate, due to the fact that the Engelund-Hansen relation may be of limited applicability to the Huanghe, but we believe that it provides a scaling estimate. That is, the result suggests that this ratio is of the order of 10.

**Table S1.** Input parameters and the resulting ratios of the properties of the channel slope, width, depth, and sediment transport capacity for the Huanghe upstream and downstream of the canyon-fan transition.

	<b>Slope [-]</b>	<b>Width [L]</b>	<b>Depth [L]</b>	<b>Sediment transport capacity [L<sup>3</sup>/T]</b>
<b>Upstream location</b>	$1.3 \times 10^{-3}$	239 m	-	-
<b>Downstream location</b>	$2.0 \times 10^{-4}$	713 m	-	-
<b>Ratio of upstream to downstream</b>	$\sim 10$	$\sim 3$	$\sim 1.1$	$\sim 50$

## 2. Computation of distance of avulsion node from Lijin

We computed the streamwise distance of the backwater-mediated avulsion nodes from Lijin using the sketch map shown in Figure 2(b). *Fan et al.* [2006] report a slightly different map than the one reported in the main text, which is shown in Figure S1. This map has a coarser resolution in time of the avulsions compared to the map modified from *Pang and Si* [1979] and *Chu et al.* [2006]. We computed the streamwise distance of the avulsion nodes from Lijin from both these maps and report the average value along with the error in Figure 3(a). Note that the map of *Fan et al.* [2006] has additional distributaries, which were not present in the map modified from *Pang and Si* [1979] and *Chu et al.* [2006]. The computed avulsion lengths (streamwise distance of the avulsion node from the shoreline) from both the maps (Fig. 2b and Fig. S2) are reported in Table S2.

**Table S2.** Comparison of the computed avulsion lengths using the map of historical avulsions from *Pang and Si* [1979] and *Chu et al.* [2006], and the map of historical avulsions from *Fan et al.* [2006]. The data points in Figure 3(a) are averages of the avulsion lengths computed from both these maps.

Channel avulsion year	Avulsion length from Fig. 2(b) [km]	Avulsion length from Fig. S2 [km]
1889	24.5	26.9
1897	27.0	31.0
1904	24.5	26.9
1917	48.3	59.9

1926	33.2	34.2
1929	25.5	26.9
1930	34.4	34.4

After computing the distance of shoreline from Lijin and the streamwise distance of the avulsion nodes from Lijin, we performed linear regression analysis on the data with their estimates of error, to determine the best-fitting lines [York *et al.*, 2004]. Further, we performed Monte Carlo error analysis for each data set where we computed 5000 linear fits between time and distance of shoreline and avulsion node from Lijin. These methods were used to determine the rate (along with the error) of shoreline migration and avulsion node migration from Lijin (Fig. 3(a)).

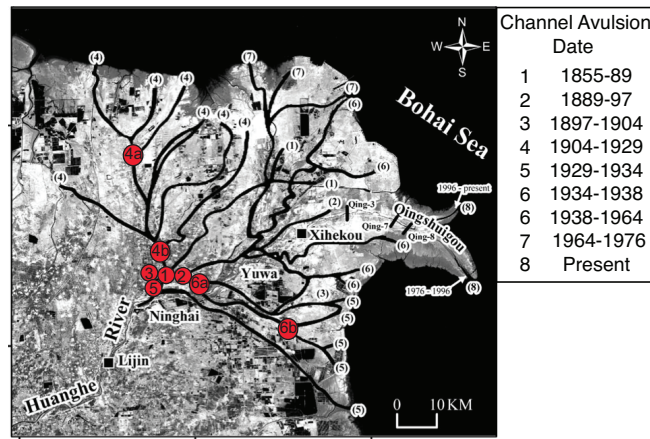


**Figure S1.** Map of backwater-mediated avulsions on Huanghe since 1855 (modified after Fan *et al.* [2006]; Xue [1994]). The numbers that mark the avulsion nodes (red circles) correspond to the channel avulsion dates in Fig. 2(b) of the main text.

### 3. Vertical aggradation rate computation

This section contains the plot showing the historical cross-sectional data (Figure S2; *Yellow River Conservancy Commission*, 2000; 2001) at three sites along the Lower Huanghe, which is used to compute the net aggradation rate  $v_a$  to estimate the channel-filling timescale  $T_c$  (see main text). We computed the net aggradation rate at all the three sites (Huayuankou, Sunkou, and Luokou) by differencing the cross-sectional data of 2001 from that corresponding to 1954, 1952, and 1951, respectively. We then averaged this aggradation over the channel cross-section and divided it by the time period under consideration to compute the in-channel aggradation rate. We note that our extrapolated value of aggradation rate at Lijin (Fig. 3b) is consistent with reported values of aggradation rates downstream of Lijin, which measure approximately 10 cm/yr [*Ru et al.*, 2008].

Moreover, due to the substantial sediment load of the Huanghe, spatiotemporal vertical aggradation rates may vary significantly, so as to increase local channel infilling that produces a site-specific avulsion. Therefore the system may be more prone to vertical aggradation than would otherwise be indicated by the cross-sectionally averaged channel cross-sections that are used to estimate  $v_a$ .

Note that we did not use the cross-section data shown in Figure S2 to compute the bankfull depth of the Huanghe and instead relied on estimates from earlier works. Previous estimates of bankfull depths of 1-3 m at Huayuankou [*Wang et al.*, 2013] closely match the observed channel depths from our compiled cross-sections at this site (Fig. S2). Cross-section data at the Lijin site (backwater mediated avulsion site) are not available, however; previous workers estimated the bankfull depths between 1.5-5 m at Lijin [e.g., *Wang et al.*, 2013].

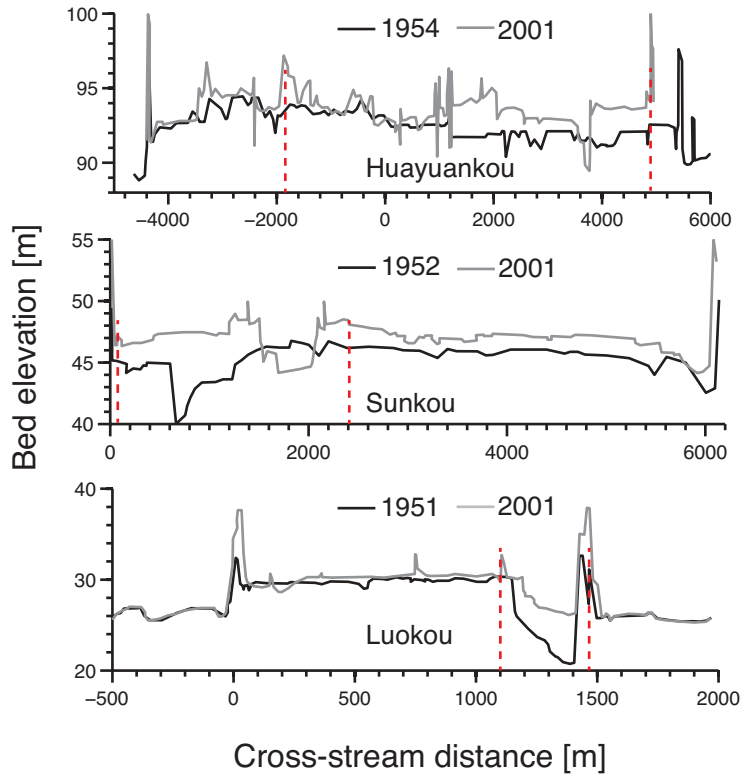


**Figure S2.** Plot showing the historical cross-sectional data used to compute the vertical aggradation rates at three sites along the lower Huanghe. (Top panel) Huayuankou site, which is ~600 km upstream of the Lijin station and corresponds to the general location of the bed-slope mediated avulsion, (Middle panel) Sunkou site, which is ~350 km upstream of Lijin site, and (Bottom panel) Luokou site, which is ~150 km upstream of the Lijin site. Note that the Huanghe is braided at the Huayuankou location (larger active channel-belt width), while it becomes a single-thread channel further downstream.

#### 4. Water discharge and stage-height variability

We compiled the historical monthly water discharge data for all the rivers considered in Fig. 3(c) to compare the water surface-elevation variability among different sites. We used the monthly water discharge data for the Rhine (Rees Station, Germany) and Rhone

(Beaucarie station, France) rivers from the River Discharge Database of the Center for Sustainability and the Global Environment, Gaylord Nelson Institute for Environmental Studies, University of Wisconsin-Madison (available at: <http://www.sage.wisc.edu/riverdata/>). The time periods of available historical monthly discharges for Rhine and Rhone were 1936-1984 (49 years) and 1920-1979 (60 years), respectively. We used the monthly water discharge data for the Orinoco (Musinacio station, Venezuela), Assiniboine (Brandon station, Canada), and Brahmaputra (Panda station, India) rivers from the Global River Discharge Database (available at: <http://daac.ornl.gov/rivdis/STATIONS.HTM#A>). The time periods of available historical monthly water discharges for Orinoco, Assiniboine, and Brahmaputra were 1970-1992 (23 years), 1906-1984 (79 years), and 1956-1979 (24 years), respectively. We used the daily discharge data for the Mississippi (Tarbert Landing station, U.S. Army Corps of Engineers) for the period between 1932-2010 (79 years), which we averaged over each month to compute the monthly average water discharge data for comparison with other rivers. Finally, the historical monthly water discharge data were available at the Lijin site on the Huanghe for the duration between 1950-2007 (58 years).

To compute the water depths from the river discharge data, we used the generalized Darcy-Weisbach relation, given by:

$$Q = wh \frac{\sqrt{ghS}}{C_f^{1/2}} \quad (5)$$

where  $Q$  is the water discharge,  $w$  is the channel width,  $h$  is the water depth,  $S$  is the topographic slope,  $g$  is the gravitational acceleration, and  $C_f$  is the nondimensional bed resistance coefficient. Rearranging equation (5) and solving for the flow depth yields:

$$h = \left(\frac{Q}{w}\right)^{2/3} \left(\frac{C_f}{gS}\right)^{1/3} \quad (6)$$

We used the values of channel width, topographic slope and friction factor reported in *Jerolmack and Mohrig* [2007], together with our compilation of the water discharges to compute the water depth variability for all the rivers under consideration in Figure 3(c). *Miao and Ni* [2009] report a coefficient of variation for streamflow between 1811-2007 at the Sanmenxia station (~200 km upstream of Huayuankou) to be 0.21, which is much smaller than that of Lijin (1.1).

Our analysis indicates that the channel-filling timescale is found to be approximately equal to the measured avulsion timescale at the bed-slope mediated avulsion node when the characteristic aggradation height used in equation (1) is  $\sim 7-9 h_c$ . Topographic cross-sectional data of the abandoned channel belt of the Huanghe reveals that the channel may have been superelevated 13 m above the outer floodplains at the bed-slope mediated avulsion node [*Chen et al.*, 2011], which is consistent with theory for large rivers that states that the appropriate length scale of aggradation used in equation (1) is likely the height of the levees with respect to the neighboring floodplain [e.g., *Heller and Paola*, 1996; *Mohrig et al.*, 2000]. However,  $T_c$  is approximately equal to  $T_{ma}$  at the backwater-mediated node when the characteristic aggradation height used in equation (1) is  $\sim 0.25 h_c$ . *Edmonds et al.* [2009] showed that avulsions in experiments occur at locations with prolonged or frequent overbank flows. To investigate whether rapid avulsions occur at the backwater-mediated node, relative to other sites in Figure 3(c), because of heightened water stage-height variability we compared the historical monthly water-surface elevation normalized by the historical record average for the rivers plotted in Figure 3(c). The monthly data at the Lijin station of the Huanghe and the

Assiniboine fan, the two outliers in Figure 3(c) (i.e.,  $T_a^*$  is significantly less than 1), show unusually high water-surface variability compared to all other rivers considered (Fig. S4; Fig 3d in main text). Additionally, the dimensionless avulsion timescale covaries with the coefficient of water stage-height variation (Fig. 3d). Our observations are consistent with the theory of *Edmonds et al.* [2009], which suggests that the low frequency of levee-overtopping flows at the bed-slope mediated node requires a high shear stress (superelevation height) to excavate a crevasse and create an avulsion. However, at the backwater-mediated avulsion node, the river aggrades less than one flow depth prior to avulsion because frequent overtopping of the levees makes levee-breaching and avulsions more likely. In addition to frequent overbank flooding, heightened water stage-height variability may affect the channel-filling processes through the transient backwater hydrodynamics (bed scour during high flow and sediment deposition during low flow) that result in an avulsion “set up” [e.g., *Chatanantavet et al.*, 2012]. Moreover, our data of water stage-height at the Huanghe delta node uses monthly-averaged discharge data, which averages over shorter-term variability influenced by tidal fluctuations. This variability can be an additional factor that may influence the avulsion timescale at the backwater-mediated node of the Huanghe.

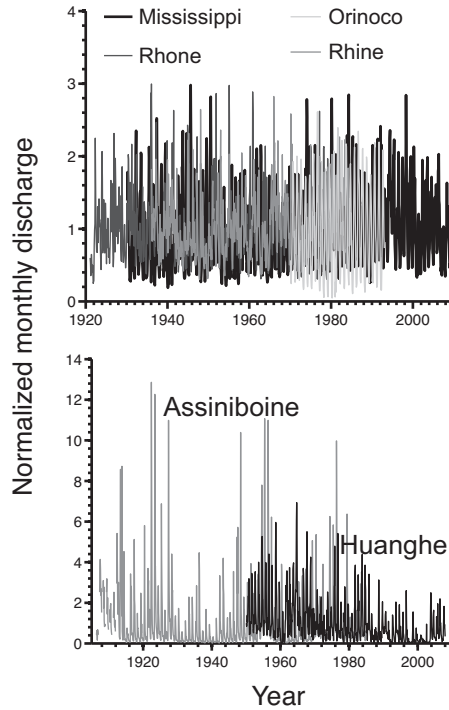


**Figure S3.** Time series of monthly discharge data normalized by their respective means for all the rivers considered in Fig. 3(c). (Top panel) Time series of river discharges for the Mississippi, Orinoco, Rhone and Rhine rivers, which show considerably less variability when compared with the time series of the monthly river discharges for the Assiniboine and the Huanghe (bottom panel).

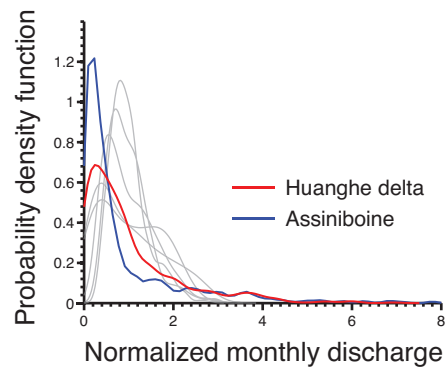


Figure S4. Comparison of the probability density functions of the monthly water surface-elevation data normalized with their respective historical means for all the rivers plotted in Figure 3(c).

## References

- Chatanantavet, P., M. P. Lamb and J. A. Nittrouer (2012), Backwater controls on avulsion location on deltas, *Geophysical Research Letters*, 39, L01402, doi:10.1029/2011GL050197.
- Chen, Y., I. Overeem, J. P. M. Syvitski, S. Gao and A. J. Kettner (2011), Controls on levee breaches on the Lower Yellow River during the years 1550-1855, *IAHS publication*, 617-633.
- Chu, Z. X., X. G. Sun, S. K. Zhai and K. H. Xu (2006), Changing pattern of accretion/erosion of the modern Yellow River (Huanghe) subaerial delta, China: Based on remote sensing images, *Marine Geology*, 227, 13-30.
- Edmonds, D.A., D. C. J. D. Hoyal, B. A. Sheets and R. L. Slingerland (2009), Predicting delta avulsions: Implications for coastal wetland restoration, *Geology*, 37, 759-762.
- Engelund, F. and E. Hansen (1967), *A Monograph on Sediment Transport in Alluvial Streams*, Teknisk Forlag, Copenhagen.
- Fan, H., H. Huang, T. Q. Zeng and K. Wang (2006), River mouth bar formation, riverbed aggradation and channel migration in the modern Huanghe (Yellow) River delta, China, *Geomorphology*, 74, 124-136.
- Heller, P. L., and C. Paola (1996), Downstream changes in alluvial architecture: An exploration of controls on channel-stacking patterns, *Journal of Sedimentary Research*, 66(2), 297-306.
- Jerolmack, D. J., and D. Mohrig (2007), Conditions for branching in depositional rivers, *Geology*, 35(5), 463-466.

- Miao, C-Y., and J-R. Ni (2009), Variation of natural streamflow since 1470 in the Middle Yellow River, China, *International Journal of Environmental Research and Public Health*, 6, 2849-2864.
- Mohrig, D., P. L. Heller, C. Paola and W. J. Lyons (2000), Interpreting avulsion process from ancient alluvial sequences; Guadalupe-Matarranya system (northern Spain) and Wasatch Formation (western Colorado), *Geological Society of America Bulletin*, 112(12), 1787–1803.
- Pang, J. Z., and S. H. Si (1979), Evolution of the Yellow River mouth: I. Historical shifts, *Oceanologia et Limnologia Sinica*, 10(2), 136-141.
- Ru, Y.Y., Wang, K.R., Hou, Z.J., 2008. Response of the reach near the Yellow River Estuary to the operation of Xiaolangdi Reservoir. *J. Sediment Res.* (3), 63–68 (in Chinese with an English abstract).
- Wang, Y., X. Fu, Y. Zhnag, and G. Parker (2013), Temporal change in bankfull characteristics of the Yellow River: Single-thread versus multiple-thread reach, *Proceedings of 2013 IAHR Congress*, Tsinghua University Press, Beijing, China.
- Xue, C. (1994), Division and recognition of modern Yellow River delta lobes, *Geographical Research*, 13, 59-66 (in Chinese with English abstract).
- Yellow River Conservancy Commission (2000), Yellow River Sediment Bulletin, Available at: <http://www.yellowriver.gov.cn/nishagonggao/>. (in Chinese).
- Yellow River Conservancy Commission (2001), Yellow River Sediment Bulletin, Available at: <http://www.yellowriver.gov.cn/nishagonggao/>. (in Chinese).

York, D., N. M. Evensen, M. López Martínez and J. De Basabe Delgado (2004), Unified equations for the slope, intercept, and standard errors of the best straight line, *American Journal of Physics*, 72, 367.